Porous Organic Cages for Gas Chromatography Separations

Adam Kewley, Andrew Stephenson, Linjiang Chen, Michael E. Briggs, Tom Hasell, and Andrew I. Cooper*

Department of Chemistry and Centre for Materials Discovery, University of Liverpool, Liverpool, L69 7ZD, United Kingdom

⑤ *Supporting Information*

The analytical or preparative separation of mixtures is a central process in chemistry. For example, mixtures of hexane isomers are produced on a large scale via catalytic isomerization and then separated to isolate the most valuable isomers.[1] Likewise, many chemical analyses rely on the separation of complex mixtures by chromatography. Improved chromatographic stationary phases and new separation media are continually being developed, but some mixtures remain challenging to separate. This is usually because the components are differentiated only by small changes in size or molecular shape.

Currently, polysiloxanes are the most common stationary phases in gas chromatography (GC) columns. However, for more complex separations, cyclodextrins are often preferred. Cyclodextrins are intrinsically chiral molecules that are available in different sizes and easily derivatized. Cyclodextrin GC columns have been optimized over a number of years to give very efficient separations and sharp chromatographic peaks, both in geometrical or in chiral separations.[2−4] Recently, there has been a search for alternatives to cyclodextrins, and one strategy has been to use porous materials. Microporous materials are suited for shape-based separations because their pore sizes are of the order of molecules (<2 nm). Hence, materials such as zeolites,[5] metal-organic frameworks (MOFs),[6] and porous organic frameworks (POFs)[7] have all been investigated as stationary phases for molecular separations. There has been particular interest recently in chiral separations, both for MOFs[8] and also for zeolites.[9] However, the insolubility of framework materials can render them difficult to use in some column formats. This is particularly true for narrow-bore columns, such as those used in GC, where it may be technically challenging to introduce particles of these insoluble frameworks. By contrast, porous organic cages[10−12] (POCs) are discrete molecules that combine a permanent pore structure with solution processability. For example, CC3 (Scheme 1) is a POC that was shown previously to shape-sort aromatic compounds[13] and to separate both krypton/xenon mixtures and chiral alcohols.[14] Here, we show that CC3 can also be used as a chromatographic stationary phase by coating it inside a standard capillary column. We show that such columns can be used for the GC separation of a range of mixtures including aromatic compounds, racemic mixtures, and branched alkanes.

Homochiral **CC3**-*R* was produced by a one-pot imine condensation of 1,3,5-triformylbenzene with (*R*,*R*)-1,2-cyclo-hexanediamine, catalyzed by trifluoroacetic acid (Scheme 1).

CC3-*R* has tetrahedral symmetry and includes four windows that are large enough to be penetrated by small molecules such as gases,[10] iodine,[15] or common organic solvents.[16] In the solid state, **CC3**-*R* packs window-to-window, resulting in a 3-D interconnected pore structure that runs through the center of each cage. This leads to high levels of permanent microporosity in the crystals after desolvation, with apparent Brunauer-Emmett-Teller surface areas (SA_{BET}) of up to 800 m^2 g$^{−1}$, depending on the level of crystallinity.[17] A distinguishing feature of **CC3**-*R* and other POCs is that they are soluble in solvents such as dichloromethane and chloroform. This allows solution processing options that are unavailable for insoluble porous networks and frameworks.[18−21] Additionally, solutions of **CC3**-*R* and its enantiomer, **CC3**-*S*, may be mixed to produce the racemate, *rac*-**CC3**, which has much lower solubility than the homochiral forms of **CC3**. This allows the formation of stable, microporous *rac*-**CC3** nanoparticles by simple mixing of two solutions.[17] The particles produced by this method have been shown to form stable suspensions of uniform crystals, ideal for depositing on the inside of columns, which would be nontrivial for macroscopic crystals or frameworks.

We used the simple and commercially scalable static method to coat **CC3**-*R* in a standard-format capillary column using a homogeneous, molecular solution of the organic cage. The resulting column was found to separate a variety of mixtures including linear alkanes and chiral alcohols or amines as shown in Figure 1 (and Supporting Information Figure S1).

The separation of chiral enantiomers can be challenging due to their identical boiling points. Separation requires favorable chiral recognition mechanisms with the stationary phase, such as hydrogen bonding, metal coordination, or inclusion.[22] **CC3**-*R* is a capable stationary phase for separating a selection of racemic mixtures, and it has a particularly high selectivity for linear 2-hydroxy alkanes (Figure 1a). These chiral molecules are difficult to separate: for example, few commercial columns have been reported to give efficient separation of *rac*-2-butanol into its constituent enantiomers with such high selectivity.

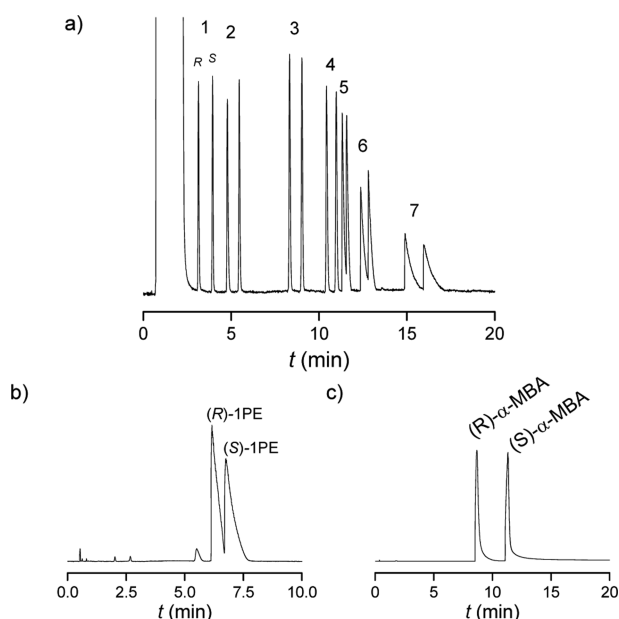**Scheme 1. Synthesis of CC3-*R***
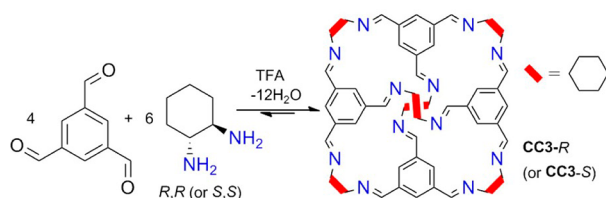
Figure 1. Separation behavior for various mixtures on a **CC3-R** column: (a) a mixture containing *rac*-2-butanol (1), *rac*-2-pentanol (2), *rac*-2-hexanol (3), *rac*-2-heptanol (4), *rac*-2-octanol (5), *rac*-2-nonanol (6), and *rac*-2-decanol (7) in diethyl ether. Only the chirality (R/S) of the 2-butanol peaks has been labeled, but the order of elution was the same for the other six chiral alcohol pairs; (b) *rac*-1-phenylethanol (*rac*-1PE); (c) *rac*-α-methylbenzylamine (*rac*-α-MBA). Additional small peaks in the chromatograms are attributed to impurities present in the samples; full details in the Supporting Information.

The separation of *rac*-1-phenylethanol was also possible using this column (Figure 1b). Selective adsorption of (S)-1-phenylethanol onto solid **CC3-R** was shown previously,[14] but we did not demonstrate any chromatographic separations. Earlier molecular simulations indicated that the chiral selectivity was a consequence of more favorable intermolecular interactions between (S)-1-phenylethanol and **CC3-R**.[14] Likewise, *rac*-α-methylbenzylamine (Figure 1c) and *rac-sec*-butylamine (Supporting Information Figure S1) can be separated into their homochiral components with the same order of elution of enantiomers as observed for the chiral alcohols, thus demonstrating that chiral recognition in **CC3-R** is not limited to just one type of compound. Based on Van't Hoff calculations (Table 1), there is a difference of 5 kJ mol^{-1} between the (R)- and (S)-1-phenylethanol association enthalpies. Similar energy differences were calculated for other chiral mixtures (Supporting Information Figure S2, Table S1). The 5 kJ mol^{-1} energy difference between (R)- and (S)-1-phenylethanol is larger than

Table 1. Thermodynamic Values Calculated from Van't Hoff Fits for 1-Phenylethanol and Hexane Isomers with CC3-R and *rac*-CC3 Columns, Respectively

	ΔH, kJ mol^{-1}	ΔS, J mol^{-1} K^{-1}
(R)-1-phenylethanol	−79.3	−134
(S)-1-phenylethanol	−84.3	−143
2,2-dimethylbutane	−44.5	−71
2,3-dimethylbutane	−50.7	−87
3-methylpentane	−61.3	−111
2-methylpentane	−65.8	−120
n-hexane	−72.8	−127

reported for a chiral POF (1.4 kJ mol^{-1}),[7] indicating that **CC3** has a stronger thermodynamic selectivity.

The substitution pattern on chiral alcohols and chiral amines determines the ability of **CC3** to separate the enantiomers. For example, while saturated 2-substituted alcohols separated on the column (Figure 1a), separation was not achieved for similar 3-substituted species, such as *rac*-3-heptanol (Supporting Information Figure S3). By contrast, unsaturated and cyclic 3-substituted alcohols, such as *rac*-1-pentyn-3-ol and *rac*-3-hydroxytetrahydrofuran, could be effectively separated (Supporting Information Figure S1).

The potential use of MOFs to separate hydrocarbons has also received much recent attention.[23] A particularly important challenge is the separation of the five structural isomers of hexane. Long and co-workers reported the separation of hexane isomers using a MOF, Fe$_2$BDP$_3$, which has triangular pores.[24] The triangular geometry was reported to be optimal for this separation, and such triangular geometries are difficult to achieve in conventional zeolites. However, a number of POCs, such as **CC3**, also have broadly triangular window shapes. This prompted us to investigate this separation where, to date, relatively few stationary phases have been successful.

Molecular separations are particularly challenging for low-functionality molecules, such as alkane isomers or aromatic isomers that differ only in shape. In such systems, comparatively weak mechanisms must be exploited, such as van der Waals surface interactions.[25] In this regard, the high surface-to-volume ratios and rigid structures of crystalline microporous materials are well suited.

Initial trials with hydrocarbon separations showed peak broadening that we ascribed to poor kinetics of diffusion of the analytes in the **CC3-R** coating. To rectify this, two modifications were made to the method. First, the amount of **CC3** coated in the column was reduced, since thinner films are known to improve diffusion kinetics and to reduce peak broadening.[26] Second, a column was produced using a suspension of preformed *rac*-**CC3** nanoparticles[17] (average diameter ≈ 100 nm), again using the static coating method. In principle, diffusion kinetics should be further enhanced by the higher surface-to-volume ratio of the nanoparticles. The resulting *rac*-**CC3**-coated column was found to perform a variety of nonchiral hydrocarbon separations with comparatively sharper peaks than the **CC3-R** column (Supporting Information Figure S4). These separations include a mixture of *o/m/p*-xylene, benzene and mesitylene (both Supporting Information Figure S5) and the five hexane isomers (Figure 2).

The *rac*-**CC3** column baseline separates all five structural isomers of hexane (Figure 2). Control experiments confirmed, as expected, that the cage material is responsible for this separation effect (Supporting Information Figure S6). Even optimized commercial columns often cannot separate all five isomers of hexane. For example, of five commercial GC columns tested, only one (BetaDEX-325, a cyclodextrin based column) could separate all five isomers. In the other four commercial columns, at least two of the hexane isomers coeluted. Moreover, the BetaDEX-325 column, which could separate all five isomers, was found to have a lower separation factor than the *rac*-**CC3** column. The relatively broad peaks in the *rac*-**CC3** column might be reduced by further optimization—for example, by reduction in the *rac*-**CC3** particle size.

The baseline separation of all five isomers compares favorably with the Fe$_2$BDP$_3$ MOF, where breakthrough experiments showed that the two dibranched isomers eluted
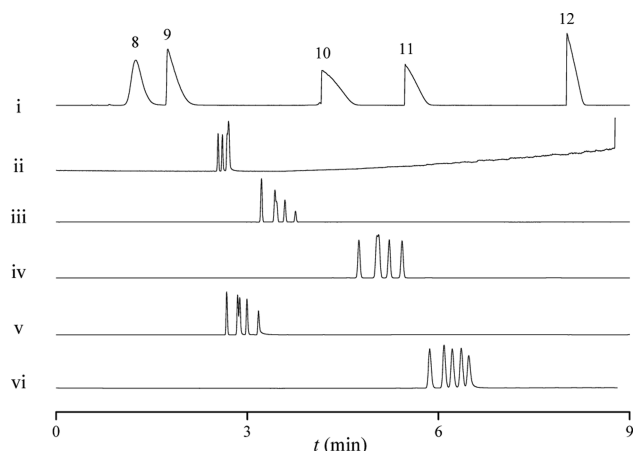
Figure 2. Separation of the five isomers of hexane using the *rac*-**CC3**-coated column and various commercial GC columns: 2,2-dimethylbutane (8), 2,3-dimethylbutane (9), 3-methylpentane (10), 2-methylpentane (11), and *n*-hexane (12); hexane isomer mixture separated with *rac*-**CC3** column (i), Chiraldex G-TA (ii), SGE-BP1 (iii), Agilent HP-1 (iv), BetaDEX-225 (v), and BetaDEX-325 (vi). All separations were attempted under identical conditions; full details in the Supporting Information.

first, followed by the two monobranched isomers, and finally by linear *n*-hexane. As such, our POC gives better separation of the dibranched hexane isomers, albeit under somewhat different conditions (the MOF separation was carried out at the higher temperature of 160 °C).[24]

The elution order corresponds to the degree of branching in the hexane isomers, with the more branched isomers eluting first. Atomistic simulations indicate that *n*-hexane is better able to maximize van der Waals surface interactions with *rac*-**CC3** by conforming to the cage's diamondoid pore structure (Figure 3a,b and Supporting Information Figure S7). Branched hexane isomers can also be adsorbed by *rac*-**CC3** cage crystals. However, they are less able to conform to the diamondoid pore structure and hence they have comparatively weaker surface interactions, thus reducing the adsorption enthalpy.

A Van't Hoff plot for the hexane isomer separation was obtained from isothermal column separations, allowing the enthalpy and entropy changes for the binding of each hexane isomer with the stationary phase to be calculated (Table 1). Adsorption enthalpies derived from atomistic simulations broadly agree with the experimental Van't Hoff plots; the linear isomer is adsorbed most strongly in *rac*-**CC3**, followed by the monobranched and then the dibranched isomers. Molecular dynamics simulations (Figure 3c) indicated that the most highly branched isomers of hexane diffuse most slowly through the pores in *rac*-**CC3**. This indicates that the separation probably involves a combination of kinetic and thermodynamic effects, where the more linear isomers of hexane diffuse more frequently into particles of *rac*-**CC3** and are more strongly adsorbed than the branched isomers, which therefore elute more quickly through the column.

The **CC3**-R and *rac*-**CC3** columns were all physically and chemically robust and were shown to be reusable (>300 injections in each case, Supporting Information Figures S8 and S9). Also, it should be noted that **CC3**-R is quite hydrolytically stable and may be boiled in water with no chemical change.[27] The solubility, functionality, and porosity of these POCs can be fine-tuned by dynamic covalent scrambling,[28] by chemical derivatization,[29] or by modular cocrystallization.[30] This, along
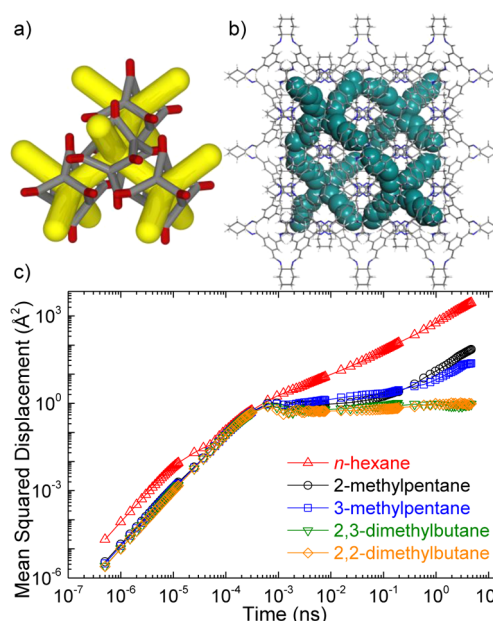

Figure 3. (a) Schematic packing diagram for **CC3**; the diamondoid pore network is illustrated in yellow; (b) Atomistic simulation suggesting most favorable positions for *n*-hexane (highlighted in green) within *rac*-**CC3**; (c) Molecular diffusion of hexane isomers in *rac*-**CC3** as obtained from molecular dynamics simulations at 298 K. The distance that each isomer diffuses through *rac*-**CC3** is plotted against time; higher displacement indicates greater average diffusion speed.

with the use of other already known POCs, has the potential to produce a wide range of stationary phases with different properties. Both cage-loaded columns were simple to produce using uncomplicated and commercially adaptable static coating methods. Just 10 mg of **CC3** is required to produce each column.

In summary, porous cage-coated capillary columns were shown to perform both chiral GC separations and also hydrocarbon GC separations using molecular sieving. For hexanes, the baseline selectivity that we observed was not achieved with four out of the five commercial GC columns tested (Figure 2). The solution processability of POCs, combined with the ability to tailor their pore size by modular assembly,[28−31] makes them interesting as next-generation stationary phases for otherwise difficult separations. Also, as these GC columns are simple to prepare and on a very small scale, they offer a convenient high-throughput platform to screen new porous molecular materials for potential preparative-scale separations.

■ ASSOCIATED CONTENT

Ⓢ Supporting Information

Full experimental materials and methods, SEM, and computational methods. This material is available free of charge via the Internet at http://pubs.acs.org.

■ AUTHOR INFORMATION

Corresponding Author

*E-mail: aicooper@liv.ac.uk.

Notes

The authors declare no competing financial interest.

■ REFERENCES

(1) Meyers, R. *Handbook of Petroleum Refining Processes*, 3rd ed.; McGraw-Hill Professional: New York, 2003.

(2) Smolková-Keulemansová, E. *J. Chromatogr. A* **1982**, *251*, 17.

(3) Szente, L.; Szejtli, J. *Adv. Drug Delivery Rev.* **1999**, *36*, 17.

(4) Del Valle, E. M. M. *Process Biochem.* **2004**, *39*, 1033.

(5) Chang, N.; Gu, Z.-Y.; Yan, X.-P. *J. Am. Chem. Soc.* **2010**, *132*, 13645.

(6) Gu, Z.-Y.; Yan, X.-P. *Angew. Chem., Int. Ed.* **2010**, *49*, 1477.

(7) Dong, J.; Liu, Y.; Cui, Y. *Chem. Commun.* **2014**, *50*, 14949.

(8) Li, J.-R.; Sculley, J.; Zhou, H.-C. *Chem. Rev.* **2012**, *112*, 869.

(9) Van Erp, T. S.; Caremans, T. P.; Dubbeldam, D.; Martin-Calvo, A.; Calero, S.; Martens, J. A. *Angew. Chem., Int. Ed.* **2010**, *49*, 3010.

(10) Tozawa, T.; Jones, J. T. A.; Swamy, S. I.; Jiang, S.; Adams, D. J.; Shakespeare, S.; Clowes, R.; Bradshaw, D.; Hasell, T.; Chong, S. Y.; Tang, C.; Thompson, S.; Parker, J.; Trewin, A.; Bacsa, J.; Slawin, A. M. Z.; Steiner, A.; Cooper, A. I. *Nat. Mater.* **2009**, *8*, 973.

(11) Zhang, G.; Mastalerz, M. *Chem. Soc. Rev.* **2014**, *43*, 1934.

(12) Xiong, M.; Ding, H.; Li, B.; Zhou, T.; Wang, C. *Curr. Org. Chem.* **2014**, *18*, 1965.

(13) Mitra, T.; Jelfs, K. E.; Schmidtmann, M.; Ahmed, A.; Chong, S. Y.; Adams, D. J.; Cooper, A. I. *Nat. Chem.* **2013**, *5*, 276.

(14) Chen, L.; Reiss, P. S.; Chong, S. Y.; Holden, D.; Jelfs, K. E.; Hasell, T.; Little, M. A.; Kewley, A.; Briggs, M. E.; Stephenson, A.; Thomas, K. M.; Armstrong, J. A.; Bell, J.; Busto, J.; Noel, R.; Liu, J.; Strachan, D. M.; Thallapally, P. K.; Cooper, A. I. *Nat. Mater.* **2014**, *13*, 954.

(15) Hasell, T.; Schmidtmann, M.; Cooper, A. I. *J. Am. Chem. Soc.* **2011**, *133*, 14920.

(16) Jones, J. T. A.; Holden, D.; Mitra, T.; Hasell, T.; Adams, D. J.; Jelfs, K. E.; Trewin, A.; Willock, D. J.; Day, G. M.; Bacsa, J.; Steiner, A.; Cooper, A. I. *Angew. Chem., Int. Ed.* **2011**, *50*, 749.

(17) Hasell, T.; Chong, S. Y.; Jelfs, K. E.; Adams, D. J.; Cooper, A. I. *J. Am. Chem. Soc.* **2012**, *134*, 588.

(18) Hasell, T.; Zhang, H.; Cooper, A. I. *Adv. Mater.* **2012**, *24*, 5732.

(19) Brutschy, M.; Schneider, M. W.; Mastalerz, M.; Waldvogel, S. R. *Adv. Mater.* **2012**, *24*, 6049.

(20) Bushell, A. F.; Budd, P. M.; Attfield, M. P.; Jones, J. T. A.; Hasell, T.; Cooper, A. I.; Bernardo, P.; Bazzarelli, F.; Clarizia, G.; Jansen, J. C. *Angew. Chem., Int. Ed.* **2013**, *52*, 1253.

(21) Jones, J. T. A.; Hasell, T.; Wu, X.; Bacsa, J.; Jelfs, K. E.; Schmidtmann, M.; Chong, S. Y.; Adams, D. J.; Trewin, A.; Schiffman, F.; Cora, F.; Slater, B.; Steiner, A.; Day, G. M.; Cooper, A. I. *Nature* **2011**, *474*, 367.

(22) Schurig, V. *J. Chromatogr. A* **2001**, *906*, 275.

(23) Herm, Z. R.; Bloch, E. D.; Long, J. R. *Chem. Mater.* **2014**, *26*, 323.

(24) Herm, Z. R.; Wiers, B. M.; Mason, J. A.; van Baten, J. M.; Hudson, M. R.; Zajdel, P.; Brown, C. M.; Masciocchi, N.; Krishna, R.; Long, J. R. *Science* **2013**, *340*, 960.

(25) Chen, B.; Liang, C.; Yang, J.; Contreras, D. S.; Clancy, Y. L.; Lobkovsky, E. B.; Yaghi, O. M.; Dai, S. *Angew. Chem., Int. Ed.* **2006**, *45*, 1390.

(26) *Gas chromatography*; Poole, C. F., Ed.; Elsevier: 2012.

(27) Hasell, T.; Schmidtmann, M.; Stone, C. A.; Smith, M. W.; Cooper, A. I. *Chem. Commun.* **2012**, *48*, 4689.

(28) Jiang, S.; Jones, J. T. A.; Hasell, T.; Blythe, C. E.; Adams, D. J.; Trewin, A.; Cooper, A. I. *Nat. Commun.* **2011**, *2*, 207.

(29) Culshaw, J. L.; Cheng, G.; Schmidtmann, M.; Hasell, T.; Liu, M.; Adams, D. J.; Cooper, A. I. *J. Am. Chem. Soc.* **2013**, *135*, 10007.

(30) Hasell, T.; Chong, S. Y.; Schmidtmann, M.; Adams, D. J.; Cooper, A. I. *Angew. Chem., Int. Ed.* **2012**, *51*, 7154.

(31) Ding, H.; Yang, Y.; Li, B.; Pan, F.; Zhu, G.; Zeller, M.; Yuan, D.; Wang, C. *Chem. Commun.* **2015**, *51*, 1976.